The Plant Cell, Vol. 16, 1575–1588, June 2004, www.plantcell.org © 2004 American Society of Plant Biologists

A Fungal Metallothionein Is Required for Pathogenicity of *Magnaporthe grisea*

Sara L. Tucker,[a,1] Christopher R. Thornton,[a] Karen Tasker,[b] Claus Jacob,[b] Greg Giles,[b] Martin Egan,[a] and Nicholas J. Talbot[a,2]

[a] School of Biological Sciences, University of Exeter, Washington Singer Laboratories, Exeter EX4 4QG, United Kingdom
[b] School of Chemistry, University of Exeter, Exeter, EX4 4QD, United Kingdom

The causal agent of rice blast disease, the ascomycete fungus *Magnaporthe grisea*, infects rice (*Oryza sativa*) plants by means of specialized infection structures called appressoria, which are formed on the leaf surface and mechanically rupture the cuticle. We have identified a gene, *Magnaporthe metallothionein 1* (*MMT1*), which is highly expressed throughout growth and development by *M. grisea* and encodes an unusual 22–amino acid metallothionein-like protein containing only six Cys residues. The *MMT1*-encoded protein shows a very high affinity for zinc and can act as a powerful antioxidant. Targeted gene disruption of *MMT1* produced mutants that show accelerated hyphal growth rates and poor sporulation but had no effect on metal tolerance. Mmt1 mutants are incapable of causing plant disease because of an inability to bring about appressorium-mediated cuticle penetration. Mmt1 appears to be distributed in the inner side of the cell wall of the fungus. These findings indicate that Mmt1-like metallothioneins may play a novel role in fungal cell wall biochemistry that is required for fungal virulence.

INTRODUCTION

Magnaporthe grisea is the causal agent of rice blast disease, the most severe disease of cultivated rice (*Oryza sativa*) and a significant constraint on worldwide rice production (Talbot, 2003). *M. grisea* causes plant infection by means of specialized infection structures called appressoria. These dome-shaped cells differentiate from the ends of fungal germ tubes and generate mechanical force to bring about rupture of the plant cuticle and entry to internal tissues (Howard et al., 1991). The biology of appressorium development in *M. grisea* has received considerable attention, and it is now apparent that a signaling pathway involving generation of cyclic AMP and the presence of a mitogen-activated protein (MAP) kinase encoded by the *PMK1* gene is required for appressorium formation to occur (Xu and Hamer, 1996; Dean, 1997).

In spite of recent progress in determining which signal transduction pathways regulate infection structure formation in plant pathogenic fungi, very little is currently known about downstream targets of these pathways and, in particular, which morphogenetic proteins are needed for appressoria to function. In this report, we describe the identification of an unusual metallothionein-encoding gene, *Magnaporthe metallothionein 1* (*MMT1*), from *M. grisea* that we identified because it showed reduced expression in a Δ*pmk1* mutant. The metallothionein encoded by *MMT1* is required for appressoria to function correctly and is necessary for fungal pathogenicity.

Metallothioneins (MTs) are small, metal binding proteins found in all eukaryotes and in several prokaryotes (Vasák and Kägi, 1983; Andrews, 2000; Blindauer et al., 2001). MTs are particularly rich in Cys residues, which are involved in binding multiple copper or zinc atoms under physiological conditions. Mammalian MTs, for example, are proteins of ~60 amino acids with 20 highly conserved Cys residues (Hamer, 1986) that tightly bind metal ions in two distinct polynuclear clusters, the α and β clusters (K_d (Zn^{2+}) = 3.2×10^{-13} M, pH 7.4) (Kägi, 1993). Based on their unusual chemical properties, MTs are implicated in a variety of physiological processes, including maintaining homeostasis of essential metals, metal detoxification, scavenging free radicals, and regulating cell growth and proliferation (Palmiter, 1998; Vasák and Hasler, 2000). Interestingly, MTs have also been implicated as possible cellular redox sensors that trigger zinc-mediated response pathways upon cluster oxidation (Fabisiak et al., 2002).

In fungi, MTs have only been sporadically investigated and are mainly classified as copper binding proteins, such as the Cup1 MT from the budding yeast *Saccharomyces cerevisiae*. *CUP1* is expressed in response to copper ions and protects yeast from copper toxicity. As a consequence, Δ*cup1* mutants are extremely sensitive to copper salts (for a review, see Hamer, 1986). Similar MTs have been described in *Neurospora crassa* (Münger et al., 1987), *Agaricus bisporus* (Münger and Lerch, 1985), and most recently in a mycorrhizal fungus (Lanfranco et al., 2002).

Here, we show that in *M. grisea MMT1* encodes an unusual MT-like protein of only 22 amino acids. Mmt1 displays a high affinity for zinc and is able to act as a powerful antioxidant because of its low redox potential and by virtue of its ability to

[1] Current address: Department of Plant Pathology, University of Arizona, Tucson, AZ 85721-0036.
[2] To whom correspondence should be addressed. E-mail n.j.talbot@exeter.ac.uk; fax 44-1392-264668.
The author responsible for distribution of materials integral to the findings presented in this article in accordance with the policy described in the Instructions for Authors is: Nicholas J. Talbot (n.j.talbot@exeter.ac.uk).
Article, publication date, and citation information can be found at www.plantcell.org/cgi/doi/10.1105/tpc.021279.

release metal in the presence of reactive oxygen species. Our results implicate MTs in cell wall differentiation in fungi and indicate that they may play an unexpected role in the developmental biology of plant pathogenic fungi.

RESULTS

Identification of a *PMK1*-Regulated MT Gene in *M. grisea*

The *M. grisea MMT1* gene was first identified as a cDNA clone that showed elevated expression in mycelium of a wild-type strain of *M. grisea* compared with an isogenic mutant lacking the *PMK1* MAP kinase gene. We reasoned that genes under control of this MAP kinase pathway (Xu and Hamer, 1996) might be important in the plant infection process by *M. grisea*. RNA gel blots confirmed that *MMT1* shows reduced expression in a Δ*pmk1* mutant under conditions of glucose starvation, as shown in Figure 1A, and also showed the 0.4-kb *MMT1* transcript to be highly abundant at all stages of fungal development, with particularly high expression during conidiogenesis (Figure 1B). Sequencing of a 392-bp cDNA clone and a 4051-bp genomic fragment spanning the *MMT1* locus revealed an open reading frame of 66 bp interrupted by a single 118-bp intron. *MMT1* putatively encodes a 22–amino acid protein, which showed 58.3% identity to a putative MT encoded by the *PIG11* gene from the bean rust fungus *Uromyces fabae*, as shown in Figure 2A. *PIG11* is highly expressed during plant infection (Hahn and Mendgen, 1997), as are two other related MT genes, *CAP3* and *CAP5* from *Colletotrichum gloeosporioides* (Hwang and Kolattukudy, 1995). The Mmt1 MT shows an unusual composition because it only has six Cys residues but resembles the N-terminal β-domain of mammalian MT, with 24% identity (Figure 2B). Mmt1 contains no hydrophobic or aromatic amino acids, in common with other MT proteins, and does not have a signal sequence or other motifs indicative of secretion or processing.

Fungal MTs have been implicated in the response of cells to toxic concentrations of metals (Butt et al., 1984). To determine whether *MMT1* was induced by metal exposure, cultures of *M. grisea* were exposed to increasing concentrations of $CuSO_4$ and RNA gel blots performed. No elevated *MMT1* expression was observed in response to copper (Figure 1C) or to other metals, including lead, cadmium, or zinc (data not shown). MTs are often induced as part of the response to environmental stress, and so *M. grisea* was exposed to heat shock, cold shock, and acute hyperosmotic stress, as shown in Figure 1D. *MMT1* was highly expressed under all conditions tested but only showed elevated expression in response to hyperosmotic stress induced by exposure to 1 M sorbitol for 24 h (Figure 1E). Interestingly, exposure to 0.5 M NaCl for the same period did not induce a similar response, indicating that only certain forms of hyperosmotic stress affect *MMT1* expression.

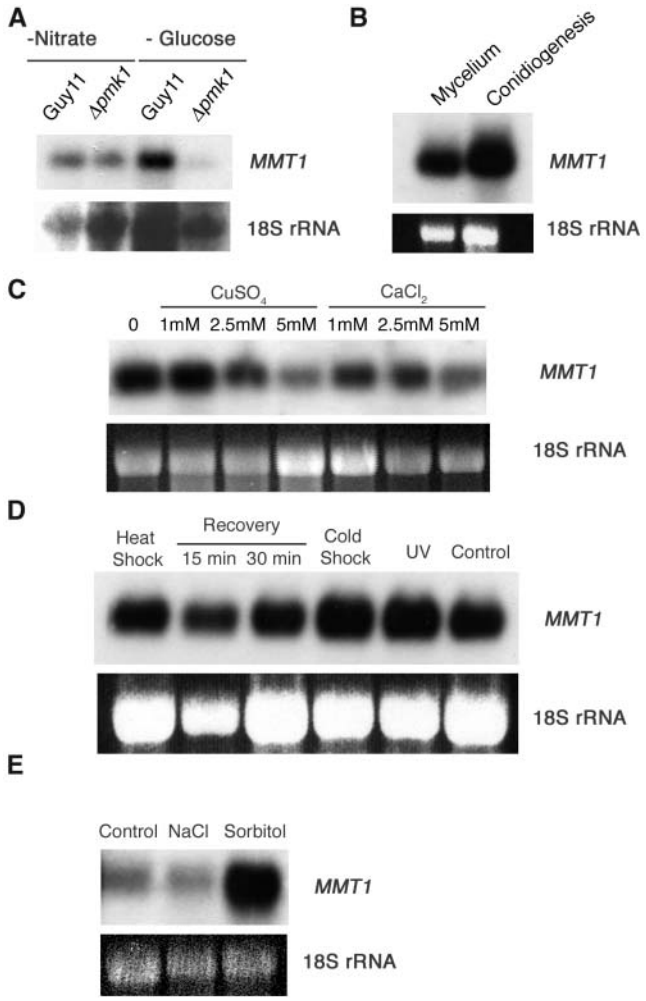

Figure 1. Gene Expression Analysis of *M. grisea MMT1*.

(A) RNA was extracted from mycelium of *M. grisea* Guy11 and Δ*pmk1* MAPK mutant nn95 exposed to conditions of glucose or nitrate starvation for 24 h. RNA gel blots were probed with the 0.4-kb *MMT1* cDNA or the rDNA probe pMG1 (Talbot et al., 1993).

(B) RNA gel blot of *MMT1* expression in conidiating (light-grown) cultures and nonconidiating (dark-grown) *M. grisea* strain Guy11.

(C) Effect of metal exposure on *MMT1* expression. Cultures of Guy11 were exposed to $CuSO_4$ or $CaCl_2$ (as a control) for 8 h.

(D) Effect of environmental stress on *MMT1* expression. *M. grisea* cultures were exposed to heat shock at 42°C for 30 min, followed by recovery for 15 min or 30 min, cold shock at 4°C, and exposure to UV (280 nm) for 30 min.

(E) Effect of acute hyperosmotic stress on *MMT1* expression. All RNA gel blots were repeated three times with identical results.

MMT1 Is Involved in Hyphal Development and Sporulation

To investigate the cellular function of *MMT1*, we performed a targeted gene disruption by introducing a 1.4-kb gene cassette bestowing resistance to the antibiotic hygromycin B into the middle of *MMT1*, as shown in Figures 3A and 3B. The gene disruption vector was introduced into a rice pathogenic strain of *M. grisea*, Guy11, and hygromycin-resistant transformants were selected. DNA gel blot analysis identified five gene disruption mutants, of which three are shown in Figure 3C. Verification that *MMT1* gene disruption had resulted in complete gene inactivation was performed by RNA gel blot analysis of *mmt1*-C6, which showed complete loss of the *MMT1* transcript (Figure 3D).

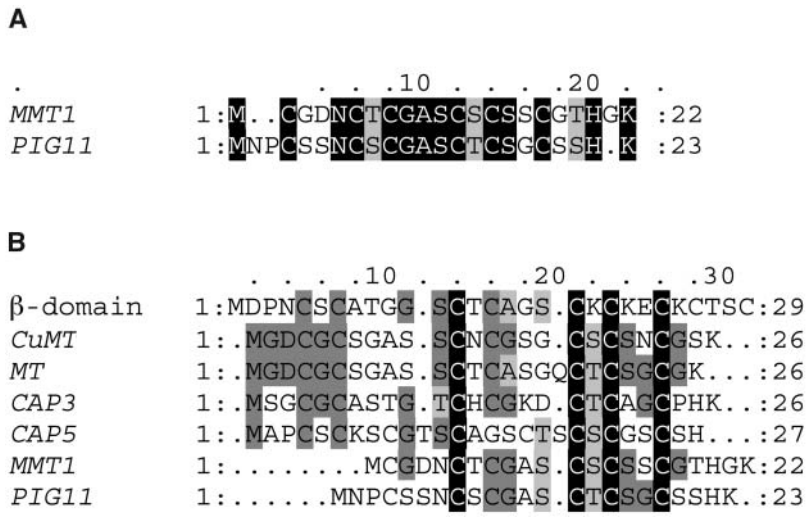

Figure 2. Predicted Amino Acid Sequence of *M. grisea* Mmt1.

(A) Sequences were aligned using ClustalW (Thompson et al., 1994). Mmt1 is aligned with the sequence of PIG11, a putative MT from the bean rust fungus *U. fabae*. Identical amino acids are highlighted on a black background, conserved amino acids on a dark gray background, and similar amino acids on light gray. Gaps are indicated by dashes.

(B) Alignment of fungal MTs with the β-domain of mammalian MT. Sequences aligned are predicted products of *M. grisea MMT1*, *U. fabae PIG11* (AAB39879), *C. gloeosporioides CAP3* (U18756) and *CAP5* (U18757), *CuMT* from *N. crassa* (X03009), and *MT* from *A. bisporus* (P04358).

The most striking phenotype of Δ*mmt1* null mutants was their ability to grow significantly faster ($P < 0.05$) than an isogenic wild-type *M. grisea* strain in plate culture, as shown in Figure 3E. This was associated with enhanced hyphal development and elongation. By contrast, conidiogenesis was dramatically reduced, and Δ*mmt1* mutants typically produced 1000-fold fewer spores compared with Guy11 ($<1 \times 10^3$ conidia per plate culture in *mmt1*, compared with 10^6 for Guy11). Mmt1 mutants also showed slightly lighter pigmentation, and because of the lack of sporulation, concentric zones of aerial hyphae were particularly apparent in plate cultures (Figure 3E). The ability of *M. grisea* to contend with exposure to metal was not affected by loss of *MMT1*. Plate tests confirmed the accelerated growth of *mmt1* mutants on all growth media tested, and when this was taken into account, no differential susceptibility of *mmt1* mutants was observed upon exposure to increasing concentrations of copper (Figure 4A), zinc, or cadmium (data not shown). Exposure to 1.5 M sorbitol did result in a significant reduction in growth of all *mmt1* mutants ($P < 0.01$), indicating that *mmt1* mutants were affected in their ability to withstand hyperosmotic stress (data not shown). Conversely, we observed that *mmt1* mutants were able to grow better after oxidative stress, either in the form of H_2O_2 or methyl viologen (paraquat), than Guy11, as shown in Figures 4B and 4C. Exposure of Guy11 to 5 mM hydrogen peroxide or methyl viologen completely inhibited its growth, whereas all *mmt1* mutants were still able to grow (Figures 4B and 4C). We conclude that *MMT1* is involved in hyphal development and conidiation in *M. grisea* but is not associated with the response to metal toxicity.

MMT1 Is Required for Plant Infection

We investigated the role of *MMT1* in plant disease by inoculating seedlings of a blast-susceptible rice cultivar, CO-39, and a blast-susceptible barley (*Hordeum vulgare*) cultivar, Golden Promise, with five independently generated *mmt1* mutants. None of the *mmt1* mutants were able to cause disease on rice or barley, and no disease lesions were observed even after prolonged incubation of the seedlings, as shown in Figure 5. Pathogenicity assays were repeated five times using 60 seedlings per experiment with uniform results. To ensure that the pathogenicity phenotype was associated with loss of *MMT1*, the gene was reintroduced and was able to restore the ability of *M. grisea* to cause disease and to grow normally (data not shown).

The ability of *mmt1* mutants to elaborate appressoria appeared normal, but we observed that appressorium-mediated cuticle penetration was severely affected ($P < 0.001$), as shown in Figure 5C. Plant infection therefore appears to be inhibited in *mmt1* strains, and consistent with this idea, we found that if the leaf cuticle was removed by abrasion, then *mmt1* mutants were able to cause disease symptoms and thus have the capacity to proliferate within plant tissue (Figure 5D). The inability to cause disease in *mmt1* mutants is thus associated with a defect in the prepenetration phase of development and traversal of the host plant cuticle.

Zinc Binding to Mmt1

To explore the biochemical properties of Mmt1, the 22–amino acid protein was synthesized and its ability to bind metal

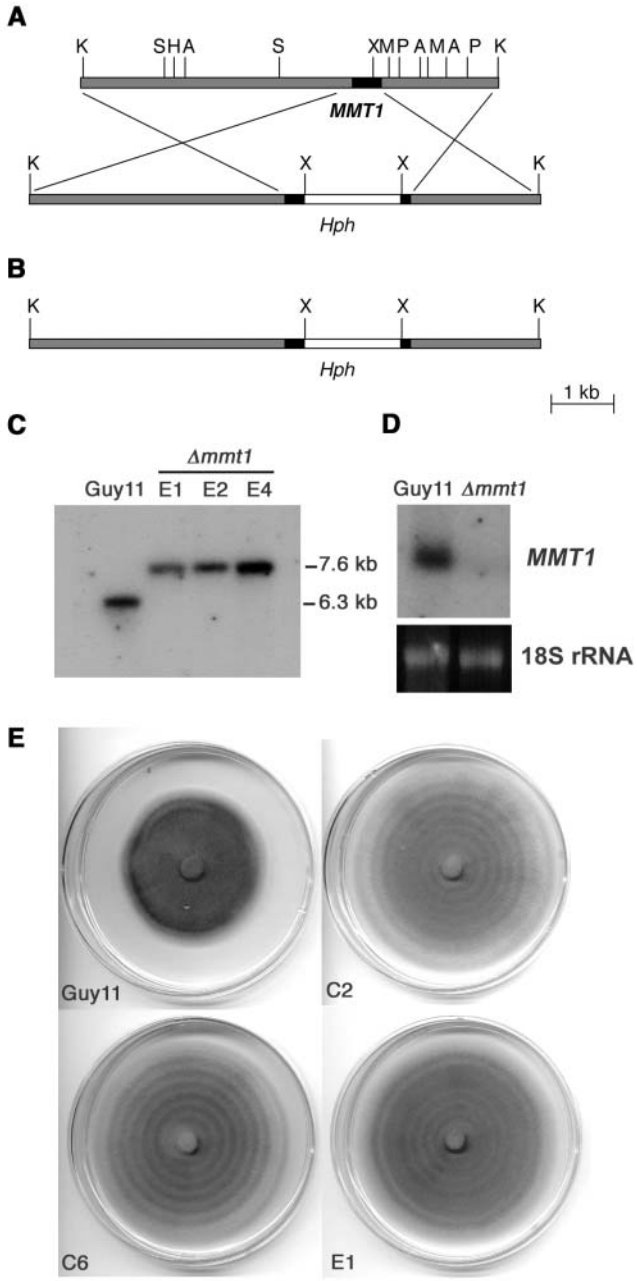

Figure 3. Targeted Gene Disruption of *M. grisea MMT1*.

(A) Restriction map of a 6.3-kb *Kpn*I fragment of the *MMT1* locus. A 1.4-kb *Xho*I fragment containing the hygromycin B resistance cassette (*Hph*) was introduced into an *Xho*I site at codon 14 of *MMT1* to create pSLT1.2H. A, *Sal*I; H, *Hin*dIII; K, *Kpn*I; M, *Sma*I; P, *Pst*I; S, *Sac*I; X, *Xho*I.

(B) The resulting 7.6-kb *Kpn*I fragment was introduced into *M. grisea* Guy11 and gene disruptants identified.

(C) DNA gel blot of pSLT1.2H transformants of Guy11 digested with *Kpn*I, fractionated by gel electrophoresis, and probed with the 0.39-kb *MMT1* cDNA. In Guy11 genomic DNA, the probe hybridized to a 6.3-kb *Kpn*I fragment spanning the MMT1 locus. In transformants E1, E2, and E4, the probe hybridized to a 7.6-kb *Kpn*I fragment, indicating that the predicted *mmt1* gene disruption had taken place.

(D) RNA gel blot of *M. grisea* Guy11 and isogenic *mmt1* mutant C6 probed with the 0.39-kb *MMT1* cDNA. RNA was extracted from mycelium grown in complete medium.

(E) Enhanced hyphal growth of *mmt1* mutants. Cultures of Guy11 and three *mmt1* mutants, C2, C6, and E1, were prepared by inoculation of a single plug of mycelium at the center of a Petri dish containing complete medium and incubated at 24°C for 10 d with a 12-h light/dark cycle.

investigated. Synthesized Mmt1 protein was added to increasing concentrations of zinc in the presence of 5,5'-dithiobis-(2-nitrobenzoic acid) (DTNB). DTNB is a thiol-specific oxidizing agent that readily reacts with the side chain of Cys residues, resulting in 5-thio-2-nitrobenzoic acid (TNB), whose rate of formation can be monitored spectrophotometrically ($\varepsilon_{412} = 13{,}600\ M^{-1}cm^{-1}$). In a control experiment containing only the non-metal-bound apothionein form of Mmt1, the Cys residues were readily oxidized by DTNB, as shown in Figure 6A. In a second control experiment, excess calcium was added to Mmt1, and Cys residues were also readily oxidized. However, after addition of 1 molar equivalent of Zn^{2+}, oxidation of the Cys residues by DTNB occurred more slowly as Zn^{2+} binding to the Cys residues slowed the oxidation reaction (Figure 6A). This was further demonstrated after Mmt1 was incubated in the presence of 1.5- and 2-fold molar excesses of Zn^{2+}. Higher concentrations of Zn^{2+} did not retard DTNB oxidation any further, suggesting that Mmt1 can bind no more than two Zn^{2+} ions per MT molecule.

To gain further insight into the zinc binding potential of Mmt1, atomic absorption spectroscopy (AAS) of the (purified) zinc form of Mmt1 was performed and predicted that on average 1.71 Zn^{2+} ions are bound per Mmt1 molecule. Two further assays were used to determine the number of zinc ions bound by Mmt1. The release of Zn^{2+} from Mmt1 by ebselen, a selenium compound that very effectively releases zinc from mammalian MT (Jacob et al., 1998a), was investigated. For this assay, Mmt1 and ebselen were incubated in the presence of the metallochromic dyes pyridylazoresorcinol (PAR) and Zincon, which form colored complexes with free Zn^{2+}, and this was used to calculate the number of protein-bound Zn^{2+} ions (Jacob et al., 1998a; Shaw et al., 1990). The average ratios of zinc ions:thiols per protein were 0.347 ($\pm$0.026) and 0.3512 ($\pm$0.039) using the PAR and Zincon assay, respectively. Multiplied by six to account for six Cys residues per protein molecule, the number of Zn^{2+} ions per Mmt1 molecule is 2.08 and 2.11 for the PAR and Zincon assay, respectively. This confirmed that the predicted number of Zn^{2+} ions bound per Mmt1 molecule is $\sim$2 as indicated by AAS.

Zinc binding was investigated further using zinc transfer from PAR (or Zincon) to apo-Mmt1 as a measure of zinc binding (data not shown). Interestingly, under the experimental conditions chosen, the decrease in absorbance at 500 nm (620 nm for Zincon) corresponded to transfer of 1.2 Zn^{2+} ions from the $Zn(PAR)_2$ complex to apo-Mmt1 (1.3 in the case of Zincon). These numbers indicate that one Zn^{2+} ion tightly binds to the protein, whereas a second zinc ion, although associated with Mmt1 (see above), is more weakly bound. This was further investigated using a pH titration experiment.

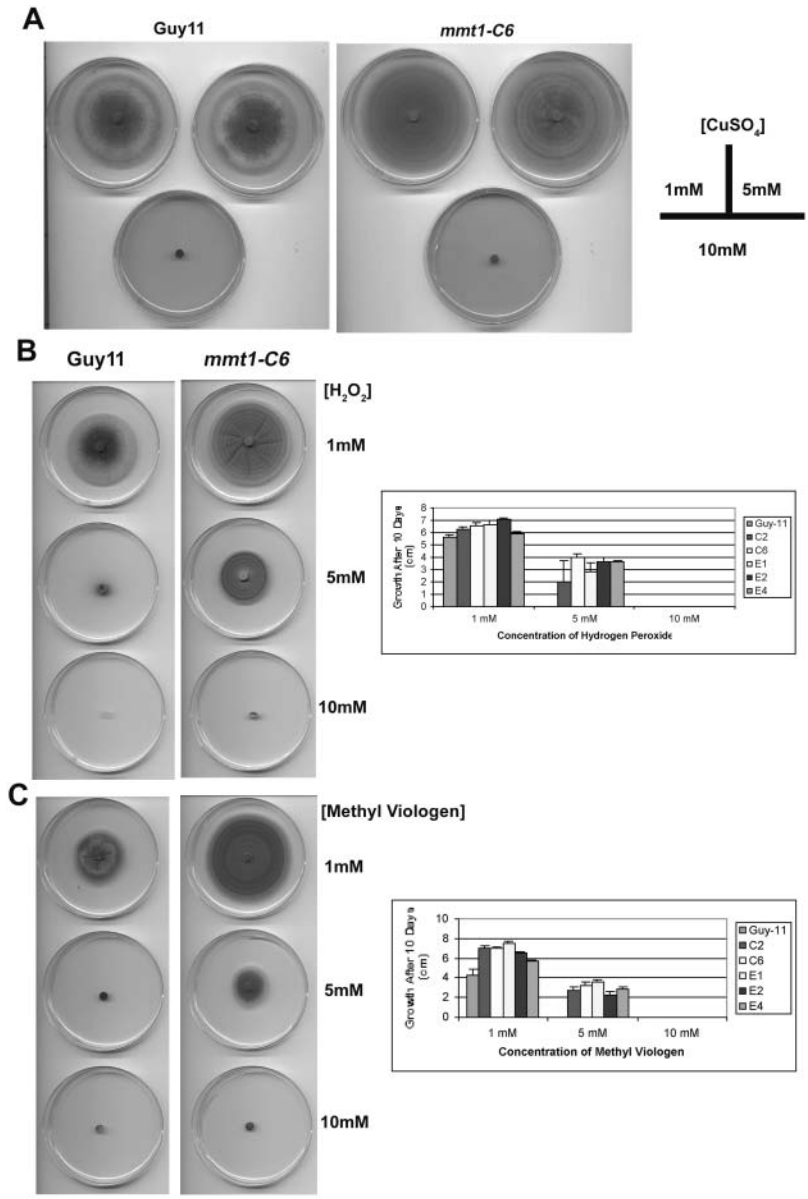

Figure 4. Phenotype Analysis of *M. grisea mmt1* Mutants.

(A) Effect of copper on vegetative growth of Guy11 and *mmt1-C6*. Complete medium was supplemented with 1, 5, and 10 mM $CuSO_4$ and growth monitored after 10 d.

(B) Effect of hydrogen peroxide on Guy11 and *mmt1* mutants. Complete medium was supplemented with 1, 5, or 10 mM H_2O_2, and growth was monitored after 10 d. The bar chart shows the results for Guy11 and five *mmt1* mutants, *mmt1*-C2, C6, E1, E2, and E4. Growth of Guy11 did not occur upon exposure to concentrations of 5 mM H_2O_2 or higher.

(C) Effect of methyl viologen (paraquat) on vegetative growth of Guy11 and *mmt1* mutants. Paraquat was added to medium and growth recorded after 10 d. The bar chart shows the results for Guy11 and five *mmt1* mutants, *mmt1*-C2, C6, E1, E2, and E4. Growth of Guy11 did not occur upon exposure to concentrations of 5 mM methyl viologen or higher.

Stability of Mmt1-Metal Protein Complexes

The chromophoric properties of metal-thiolate complexes of MT provide a means to assess the stability of the metal-protein complex by pH titration. Displacement of zinc by protons results in a decrease of absorbance at 220 nm, reflecting a charge transfer of the Zn-S (Cys) bond (Vasák and Kägi, 1983). For previously purified MTs, such titrations have resulted in a sigmoidal curve as the protein moves from a weak to a strong binding state (Vasák and Kägi, 1983; Jiang et al., 2000). In the case of Mmt1, a sigmoidal curve was also observed, as shown in Figure 6B, but there is a slight dip in the curve around pH 6.0,

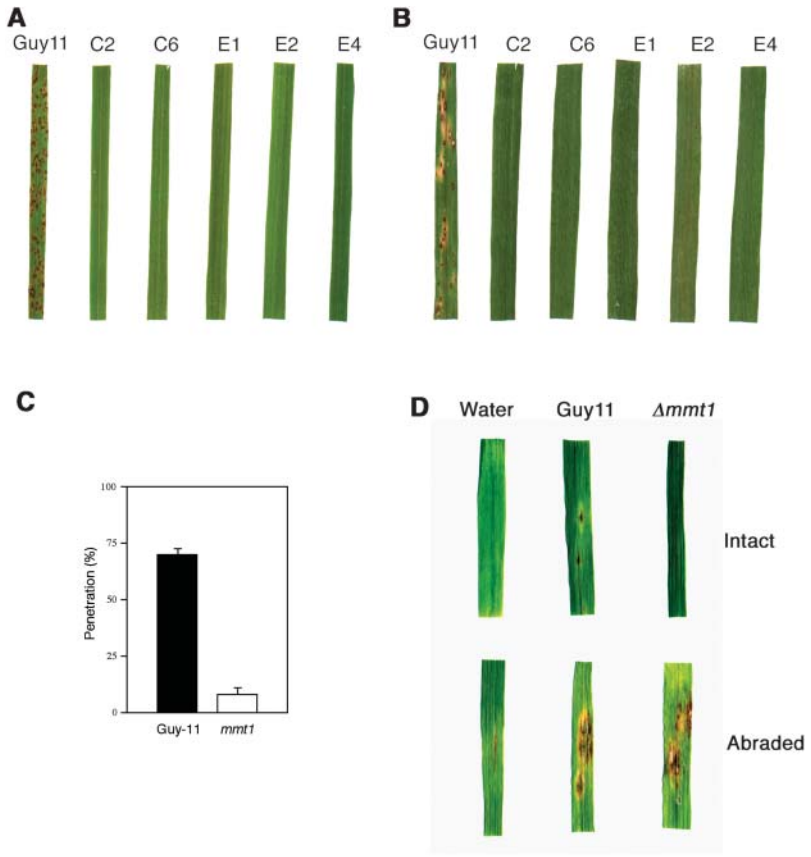

Figure 5. Virulence Phenotype of *M. grisea mmt1* Mutants.

(A) Seedlings of rice cultivar CO-39 were inoculated with *M. grisea* conidial suspensions of identical concentration (1×10^5 conidia mL^{-1}) of strain Guy11 and *mmt1* mutants C2, C6, E1, E2, and E4. Seedlings were incubated for 4 d for development of blast disease.
(B) Identical virulence assays using blast-susceptible barley cultivar Golden Promise.
(C) Bar chart showing ability of appressoria of Guy11 and *mmt1* mutant C6 to elaborate penetration hyphae after 24 h ($n = 200$, bars = SD).
(D) Effect of cuticle removal on pathogenicity of *mmt1* mutants. Barley leaf sections were lightly abraded with fine sandpaper to remove cuticle and a conidial suspension (1×10^3 conidia mL^{-1}) of Guy11 or *mmt1*-C6 incubated on the leaves for 6 d. Controls were intact and mock-inoculated leaves.

which may be caused by the presence of a His residue in Mmt1. The absorbance remains virtually constant above pH 7.0 but decreases sharply in a narrow range between pH 3.0 and 5. From this pH titration curve, it was possible to estimate the Zn binding constant for Mmt1, accounting for two alternative binding models. If zinc ion is bound in a Zn_2Cys_6 cluster by two end-on and two bridging Cys, then the K_d (Zn^{2+}) would be in the order of 8×10^{-25} M. Alternatively, if the two zinc ions are bound in two separate complexes [i.e., one $ZnCys_4$ and one $ZnCys_2His(H_2O)$ coordination], then K_d (Zn^{2+}) would be around 1.0×10^{-21} M. It must be pointed out, however, that these numbers are indicative of the strongest bound Zn^{2+} ion and do not take the possible weaker binding site into account. The structural details of zinc binding and the subsequent determination of a more precise zinc binding constant are therefore currently under investigation. At this stage, a binding model with one $ZnCys_4$ and one $ZnCys_2His(H_2O)$ site is consistent with the experimental data presented.

Zinc Release from *M. grisea* Mmt1 during Oxidative Stress

There is evidence that MTs release bound metals during oxidative stress (Fliss and Ménard, 1992; Maret, 1994), and we reasoned that this might be a potential role for the *MMT1*-encoded MT in *M. grisea*. Plant defense can be accompanied by release of reactive oxygen species, which accumulate rapidly at the sites of fungal infection (Lamb and Dixon, 1997; Mellersh et al., 2002). Oxidation of metal-thiolate clusters suggests that MTs could act as scavengers of deleterious oxygen radicals (Thornalley and Vasák, 1985; Palmiter, 1998) and trigger a Zn-mediated antioxidant response (Andrews, 2001). To determine whether Mmt1 would relinquish bound metal during oxidative stress, an experiment was undertaken to measure the rate at which zinc was released from Mmt1 in the presence of H_2O_2. Mmt1 was incubated with $ZnSO_4$ overnight to ensure complete metal binding to the MT. Excess $ZnSO_4$ was then removed by passing Mmt1 through a gel filtration column and mixing the purified

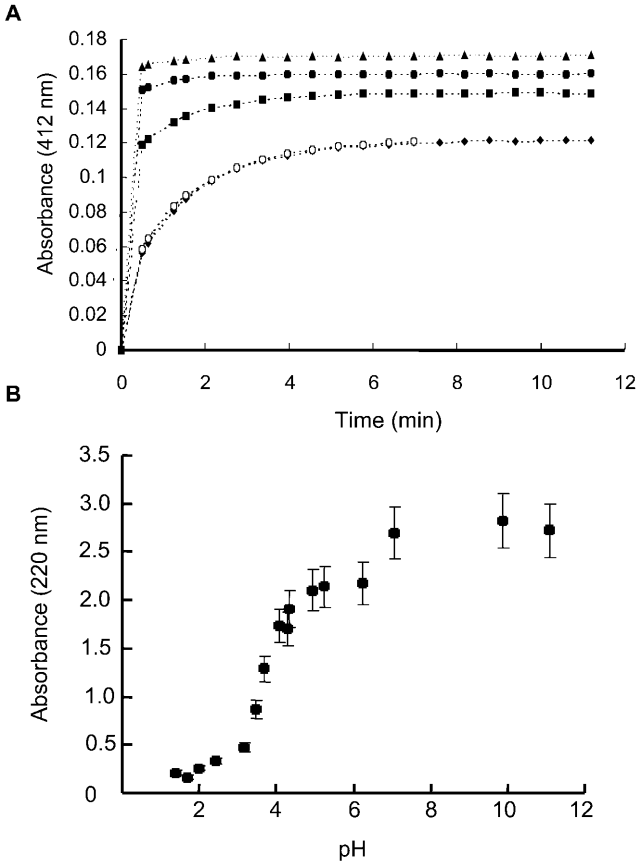

Figure 6. Zinc Binding to Mmt1.

(A) The apo-form of Mmt1 (2 μM) was incubated with DTNB (100 μM) in Hepes buffer (nitrogen purged, 25°C) and thiol oxidation monitored spectrophotometrically at 412 nm. As the concentration of metal ions in the solution increased, the rate at which this oxidation occurred slowed, indicative of metal binding to Mmt1, which interferes with thiol oxidation. Closed triangle, apo-Mmt1; closed circle, $CaCl_2$ control (4 μM); closed square, 2 μM $ZnSO_4$; closed diamond, 3 μM $ZnSO_4$; open circle, 4 μM $ZnSO_4$.

(B) Stability of metal-thiolate complexes of Mmt1 assessed by pH titration. Formation of the thiolate-zinc bond results in an increase of absorbance at 220 nm, measured spectrophotometrically. Apo-Mmt1 (2 μM) was dissolved in 0.1 M $NaClO_4$, pH 7. The pH of the solution was adjusted to 1.8 with $HClO_4$, and 4 μM of $ZnSO_4$ was added. At this low pH, the metal would not bind to the MT. The pH was then increased with NaOH (10, 50, and 100 mM) and changes in absorbance measured at 220 nm. The resulting pH profile was used to estimate the magnitude of metal binding to the protein. Values represent mean of three independent experiments. Bars = SD.

protein with PAR. This metallochromic dye acts as a zinc acceptor, and by following the reaction spectrophotometrically, it was possible to detect formation of the $Zn(PAR)_2$ complex (Shaw et al., 1990) as metal was released from the MT. Figure 7A shows that after addition of 1 mM H_2O_2, Zn^{2+} is gradually released by Mmt1 and becomes bound to PAR, resulting in a color change that is detected spectrophotometrically at 500 nm and is shown in Figure 7A as a curve. To determine the maximum zinc release from Mmt1, the protein was incubated under the same experimental conditions but in the presence of ebselen (Jacob et al., 1998a) to effectively liberate all bound Zn^{2+}. After 50 min in the presence of H_2O_2, 45% of the bound zinc was released by Mmt1 and transferred to PAR, whereas Mmt1 did not relinquish any metal, as shown in the control experiment (Figure 7A). This indicates that Mmt1 is able to act as antioxidant by reacting with peroxide and releasing zinc. It also confirms that Mmt1 binds zinc tightly.

Mmt1 Is a Powerful Antioxidant

The redox behavior of Mmt1 was investigated in solution using cyclic voltammetry and a dropping mercury electrode (see Methods). Figure 7B shows that electron transfer from Mmt1 is reversible (Epa = −651 mV, Epc = −669 mV, E_{Mmt1} = −660 mV, all potentials given versus the standard Ag/AgCl electrode). This redox behavior is indicative of the thiol/disulfide redox couple on mercury and resembles the behavior of human MT (Olafson, 1998). To confirm thiol redox chemistry and establish a biochemically useful redox reference, GSH was tested under the same experimental conditions. GSH also shows reversible redox behavior (Epa = −488 mV, Epc = −508 mV, E_{GSH} = −498 mV) with a similar ΔE value (this corresponds to approximately −276 mV versus normal hydrogen electrode, in line with a literature value of −250 mV versus normal hydrogen electrode). The redox potential of Mmt1 is therefore more negative (reducing) than the GSH/GSSG couple, resulting in E_{Mmt1} = −162 mV versus the GSH/GSSG reference couple. The electrochemical studies show that reduced Mmt1 is an unusually strong reducing agent (when compared with other thiols) that could act as a powerful antioxidant.

Cellular Localization of Mmt1

To understand the likely function of Mmt1 during plant infection, we set out to determine the cellular location of Mmt1. A polyclonal antibody was raised to Mmt1, affinity purified, and used in immunogold transmission electron microscopy of ultrathin sections of *M. grisea* hyphae and infection structures, as shown in Figure 8. Mmt1 was located at the cell periphery of hyphae (Figures 8A and 8B), in the appressorium cell wall (Figures 8C and 8D), and in the cell wall of germ tube tips before appressorium development (Figure 8E). Cytoplasmic localization of Mmt1 was also observed, but most protein accumulated at the inner side of the cell wall in all sections observed. A control experiment without primary antibody did not reveal protein localization (Figure 8F). To ensure that the Mmt1 antibody did not cross-react with other cell wall components, the specificity of the antibody was determined by ELISA and immunoblotting. For ELISA, a second MT, Mmt2, was identified from *M. grisea*. Mmt2 represents the protein showing closest similarity to Mmt1 in the *M. grisea* genome. The gene encoding this MT was sequenced, and a synthetic peptide corresponding to Mmt2 was used to test for cross-reactivity. No cross-reaction was observed, indicating that the Mmt1 antibody is specific to Mmt1 (Figure 8G). In immunoblotting experiments, the anti-Mmt1 antibody was found to react specifically to a 26-kD protein band in protein extracts

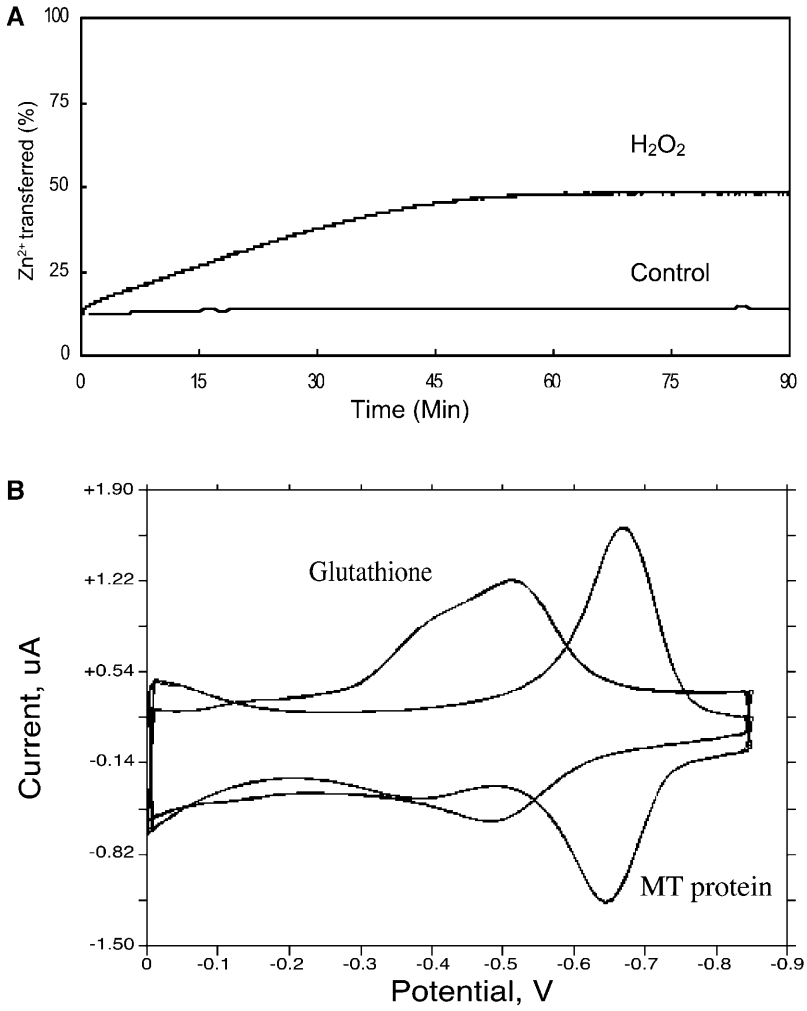

Figure 7. Antioxidant Properties of Mmt1.

(A) Reaction of hydrogen peroxide with Mmt1. The Mmt1 protein was incubated overnight in the presence of $ZnSO_4$. Hydrogen peroxide (1 mM) was added to 2 μM zinc-bound Mmt1 in the presence of 100 μM PAR in Hepes buffer (20 mM). The reaction was monitored spectrophotometrically at 500 nm for 90 min. Maximum zinc release from Mmt1 was calculated by incubation of zinc-bound Mmt1 (2 μM) with 50 μM Ebselen (Jacob et al., 1998a) under the same experimental conditions.

(B) Electrochemical redox potential of Mmt1. Zinc-bound Mmt1 (7.4 μM) was added to 100 mM KPi, pH 7.5 (N_2 purged). Comparative analysis with GSH (68 μM) was performed under identical conditions. Measurements were made at a scan rate of 800 mV s^{-1} using a BAS controlled growth mercury electrode coupled to an electrochemical analyzer, BAS100B/W. Electrochemical scans were recorded using the U.S. convention.

from hyphae of *M. grisea*. This protein band was absent in protein extracts of the *mmt1* mutant (Figure 8H). The reaction of the anti-Mmt1 antibody to a 26-kD protein indicates that the 22–amino acid protein is part of a larger multiprotein complex when extracted from cells of *M. grisea*.

Localization of Mmt1 at the cell wall prompted us to examine the structural characteristics of cell walls of *mmt1* mutants. To test the relative integrity of cell walls, we exposed hyphae of Guy11 and the *mmt1* mutant C6 to cell wall–degrading enzymes and monitored the release of protoplasts over time, as shown in Figure 9. We found that the *mmt1* mutant was hypersensitive to protoplasting enzymes, indicating a lack of structural integrity in the cell wall compared with a wild-type *M. grisea* strain.

DISCUSSION

MTs are ubiquitous Cys-rich proteins associated with numerous cellular functions, including regulation of metal homeostasis in cells and the response to metal toxicity and oxidative stress (Hamer, 1986; Palmiter, 1998). Targeted mutation of MT-encoding genes in multicellular eukaryotes, however, has often had little effect on fitness and has not proved particularly illuminating in determining MT function (for commentary, see Palmiter, 1998). In fungi, MTs have been proposed to be primarily involved in the response to metal toxicity or as general stress proteins. This study has shown that MTs may play an unexpected role in fungal virulence, allowing a plant pathogenic fungus to conduct infection-related development.

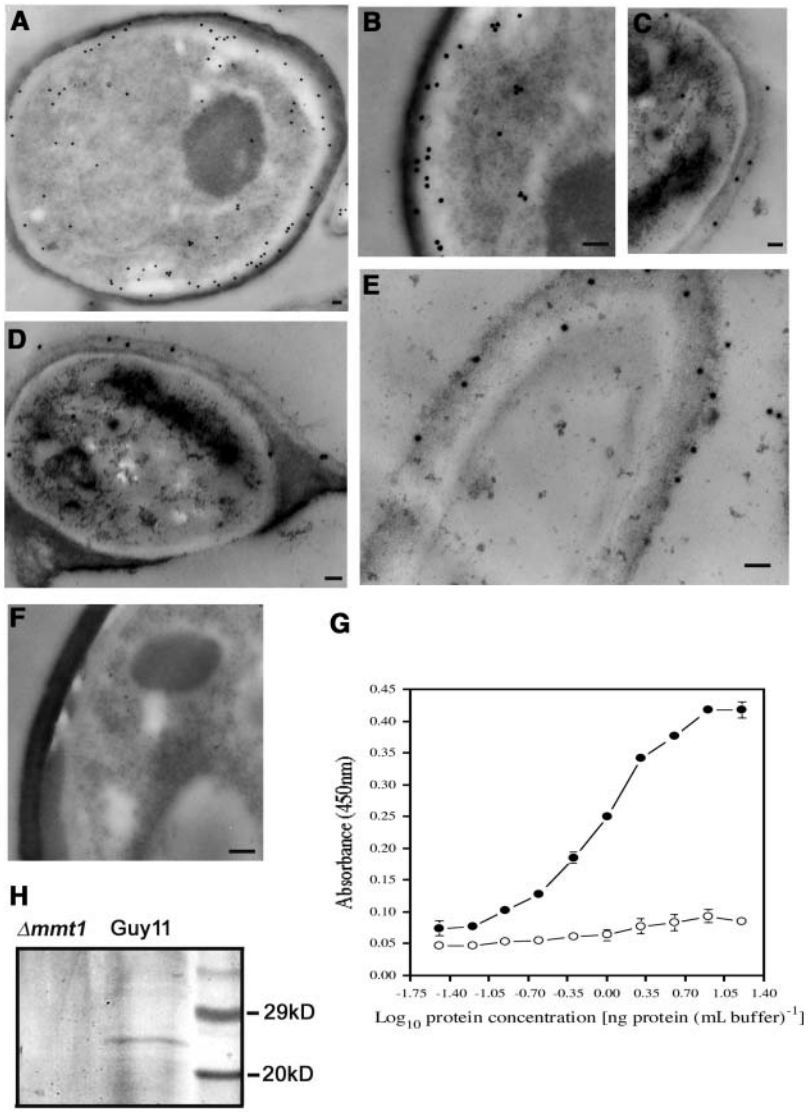

Figure 8. Cellular Localization of Mmt1 in *M. grisea*.

(A) Transmission electron micrograph showing a transverse section of a hypha of *M. grisea* Guy11 incubated with anti-Mmt1 pAB and anti-rabbit immunoglobulin 20-nm gold particles. Mmt1 was observed cytoplasmically but was also strongly associated with the inner side of the hyphal cell wall.
(B) Detail of hyphal section showing cell wall localization of Mmt1.
(C) Transverse section of the cell wall of an appressorium prepared on barley epidermis.
(D) Transverse section of a 24-h-old appressorium showing localization of Mmt1 in the cell wall.
(E) Longitudinal section of a germ tube tip, 4 h after conidial germination, before appressorium development, showing localization of Mmt1 in the apical cell wall.
(F) Transverse section of *M. grisea* hypha, incubated with anti-rabbit immunoglobulin 20-nm gold particles in absence of the primary antibody. Bar = 100 nm for **(A)** to **(F)**.
(G) ELISA showing reaction of anti-Mmt1 pAB to dilution series of Mmt1 MT (closed circles) and Mmt2 MT (open circles). Each data point represents mean of three independent replications of the experiment. Error bar represents standard error of the mean.
(H) Immunoblot showing reaction of the anti-Mmt1 antibody to a 26-kD protein band in a protein extract of the wild-type *M. grisea* strain Guy11 and the absence of this reaction to protein extracts from *mmt1* mutant E4. Each well received identical amounts of protein (2 μg per well). The size markers are broad-range prestained markers (Bio-Rad).

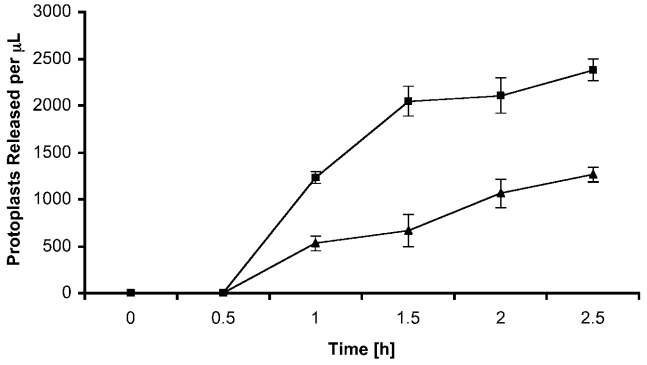

Figure 9. Hypersensitivity of *mmt1* Mutants to Cell Wall–Degrading Enzymes.

M. grisea mycelium was grown in CM broth for 48 h, recovered by filtration, and incubated with glucanex at 30°C in osmotically stabilized buffer. Protoplast release from digested mycelium was observed by microscopy. Data points shown as closed squares are *mmt1-C6*, and closed triangles are Guy11. Each data point represents mean of three replicates. Bars = SD.

To understand this unusual kind of biological activity, we studied different properties commonly associated with MTs, such as gene expression in response to metal ions, antioxidant properties, zinc storage, and metal release. *MMT1* was highly expressed in *M. grisea* at most stages of its life cycle but did not show any difference in transcript abundance in response to copper, zinc, or other metals tested. This is unusual for a fungal MT because *CUP1*, *N. crassa CuMT*, *A. bisporus MT*, and *GmarMT1* from *Gigaspora margarita* all showed induction by copper exposure (Münger and Lerch, 1985; Münger et al., 1987; Lanfranco et al., 2002). By contrast, *MMT1* expression was associated with cellular differentiation and exposure to hyperosmotic growth conditions, a stress that is also likely to involve changes in cell wall structure (Gustin et al., 1998). Gene disruption of *MMT1* produced mutants with unusual growth characteristics. Conidiogenesis was drastically reduced, and *mmt1* mutants instead produced extensive hyphal growth. Mmt1 mutants were also not affected in metal tolerance, indicating that this particular MT has little to do with the cellular response to metal toxicity.

To learn more about Mmt1, we investigated the biochemistry of the protein. Originally, we overexpressed *MMT1* in *Escherichia coli* as a glutathione *S*-transferase fusion protein, and although we succeeded in purifying small amounts of protein (data not shown), the unusual biochemical characteristics of MT precluded large-scale purification of the peptide. Instead, as a result of its size, we elected to synthesize Mmt1, and this allowed us to investigate its properties in far greater detail. In many ways, Mmt1 acted as a typical MT, in spite of its very small size and unusually low number of Cys residues. In this regard, Mmt1 showed a very high affinity for zinc, and it is likely that each Mmt1 molecule binds two atoms of zinc, in either a binuclear Zn_2Cys_6 cluster or in one $ZnCys_4$ and one $ZnCys_3His(H_2O)$ site.

Metal binding experiments were all performed using zinc because of the redox activity of copper. In most proteins, however, Cu^+ and Zn^{2+} are interchangeable, so it is likely that Mmt1 may be able to bind either metal in vivo (Thornalley and Vasák, 1985). The lack of transcriptional regulation by copper, however, indicates that unlike other fungal MTs described to date, Mmt1 may not be produced specifically to bind copper.

The DTNB and H_2O_2 assays also showed that Mmt1 has the capacity to act as an antioxidant with a very low redox potential (this is particularly true for the apo-form). It has been suggested that MTs may selectively release zinc within cells in response to local changes in the redox environment with important consequences within a cell. Zinc is not a Fenton-active metal, so this would not have deleterious effects. Zinc may become available for synthesis of antioxidant metalloproteins, such as Cu,Zn-superoxide dismutase, and at the same time be part of a mechanism that conducts spatial regulation of the oxidoreductive environment in the cell (Maret, 1994). If Mmt1 binds copper in vivo, it might also be a means of preventing Fenton-type reactions from occuring that release damaging hydroxyl radicals that can damage proteins, lipids, and nucleic acids. This activity might conversely explain the increased tolerance of *mmt1* mutants to H_2O_2 and methyl viologen. Adding a very large excess of H_2O_2, or agents that generate it, to a wild-type strain of *M. grisea* might cause copper-bound Mmt1 to contribute to the toxicity of H_2O_2 by causing release of its bound copper (as performed experimentally with H_2O_2 and zinc in Figure 7A), thereby forming Fenton-derived hydroxyl radicals. In its absence, it is possible that *M. grisea* can withstand H_2O_2 exposure more easily because of the absence of the MT in the cell wall. A key future goal will be to determine whether zinc, copper, or either metal are bound to Mmt1 in vivo.

The Role of *MMT1* in Fungal Pathogenicity

Targeted gene disruption of *MMT1* prevented *M. grisea* from causing disease. In addition, *mmt1* mutants showed rapid hyphal development but poor sporulation. Based on our biochemical studies and the mutant phenotypes observed, we believe that there are two potential roles for Mmt1 in the rice blast fungus.

The first possibility is that Mmt1 is required as a potent antioxidant to allow the fungus to withstand plant defense mechanisms that can involve a rapid oxidative burst. Release of reactive oxygen species by plants is one of the first responses of plant species to fungal infection (Mellersh et al., 2002). In rice blast infections, reactive oxygen species have been identified even at the leaf surface after inoculation with *M. grisea* spores (Pasechnik et al., 1998). The action of an MT acting at the cell periphery would provide a means of counteracting such an environment by the fungus during plant infection.

Several lines of evidence, however, argue against this model. First of all, wounding rice leaves by removal of the cuticle allowed *mmt1* mutants to grow normally in plant tissue. Wounding is likely to induce release of reactive oxygen species such that the internal plant tissue is likely to be a more stressful oxidative environment than the leaf surface. Second, *mmt1* mutants appear more tolerant of H_2O_2 and methyl viologen (paraquat)

than the wild-type strain of *M. grisea*. Finally, this model does not explain the unusual growth characteristics of *mmt1* mutants.

The second model, which we favor, suggests that Mmt1 is involved in cell wall biochemistry and, in particular, is required for cell wall differentiation in the appressorium. Several lines of evidence imply such a function. Accelerated hyphal growth of *mmt1* mutants was associated, for example, with substantially weaker cell walls because *mmt1* mutants showed hypersensitivity to protoplasting enzymes. Furthermore, loss of Mmt1 led to a drastic reduction in spore production and an inability of appressoria to elaborate penetration hyphae. Thus, both of the morphological phenotypes associated with *mmt1* mutants were associated with differentiated cell types—spores and appressoria—both of which have highly specialized cell walls in comparison with vegetative hyphae. Expression studies also showed *MMT1* to be preferentially expressed during hyperosmotic stress adaptation, a process that involves cell wall remodeling, and *mmt1* mutants were affected in their ability to withstand hyperosmotic stress. Finally, the immunolocalization of Mmt1 to the cell walls of germ tubes and appressoria of *M. grisea* is also consistent with a role for the protein in cell wall biochemistry.

Cell wall maturation during conidiogenesis and appressorium development are likely to involve cell wall thickening and melanin deposition. It would seem likely that proteins would need to become incorporated into the cell wall glucan/chitin matrix during these developmental transitions. Oxidative cross-linking of proteins is well known in plant cell wall biochemistry (Lamb and Dixon, 1997) but less described for fungi. An MT could play a key role in such a process. Formation of H_2O_2 in the fungal cell wall in the presence of an MT might, for example, cause metal release for use by metalloenzymes and allow the MT to become cross-linked via disulfide bridges into the cell wall matrix. The observation that the anti-mmt1 antibody recognizes a 26-kD protein in total protein extracts of the fungus provides some preliminary evidence that the 22–amino acid Mmt1 peptide has the capacity to aggregate with other proteins. At the same time, during the process of oxidative cross-linking, the MT could act as an electron donor/oxygen atom acceptor, detoxifying reactive oxidizing species (six thiols donate six electrons when forming disulfides and can accept up to 18 oxygen atoms).

Melanin biosynthesis in *M. grisea* is an important component of appressorium formation (de Jong et al., 1997), and melanin biosynthetic mutants produce nonfunctional appressoria and are therefore nonpathogenic (Chumley and Valent, 1990). Melanin biosynthesis occurs through a pentaketide pathway from acetyl CoA to 1,8-dihydroxynaphthalene. This diphenol is oxidized and polymerized by laccases (*p*-diphenol:oxygen oxidoreductases), cuproenzymes that are secreted by fungi. Copper-depleted inactive laccases can take up the metal and recover activity if copper salts are added to growth medium (Galhaup and Haltrich, 2001). It is therefore possible that Mmt1 plays a fundamental role in oxidative cross-linking in the cell wall but might at the same time free metal ions to promote melanin polymerization in spores and appressoria. Mmt1 may therefore contribute to cell wall differentiation and melanization of appressoria in such a way that *mmt1* mutants are prevented from forming functional appressoria. The lighter pigmentation of mmt1 mutants points to a potential role for the MT in melanin deposition, although efforts to restore virulence to the *mmt1* mutant using melanin biosynthetic intermediates have not proven successful (data not shown).

We are aware that this novel role for an MT raises many questions. How, for example, is such a small peptide carried to the cell wall in the absence of a signal peptide for conventional secretion (the peptide itself being no larger than many signal peptide sequences)? What is the cytoplasmic function of Mmt1, and does it also contribute to regulation of the intracellular redox environment? What is the structure of cross-linked MT? And finally, how are MTs used in the different growth forms of *M. grisea*? Answering these questions is in progress and will be fundamental to understanding how MTs contribute to fungal virulence.

METHODS

Fungal Strains, Growth Conditions, and DNA Analysis

Magnaporthe grisea maintenance, media composition, nucleic acid extraction, and transformation were all as described previously (Talbot et al., 1993). Gel electrophoresis, restriction enzyme digestion, gel blots, and sequencing were performed using standard procedures (Sambrook et al., 1989).

Identification and Targeted Gene Disruption of *MMT1*

MMT1 was identified using differential cDNA screening as described previously (Viaud et al., 2002). A 0.39-kb cDNA clone of *MMT1* was selected from a cDNA library derived from glucose-starved Guy11 mycelium (Xu and Hamer, 1996). A corresponding genomic clone spanning the *MMT1* locus was selected from a Guy11 λGEM-11 genomic library (Talbot et al., 1993) and subcloned as a 6.3-kb *Kpn*I fragment into pGEM-3Z to create pSLT1.2. Restriction enzyme mapping of pSLT1.2 revealed a unique *Xho*I site at codon 14 in *MMT1*. A 1.4-kb fragment containing the *Hph* gene (Carroll et al., 1994) was inserted into this *Xho*I site, creating the gene disruption vector pSLT1.2H. A 7.6-kb *Kpn*I fragment was excised from pSLT1.2H and used to transform protoplasts of Guy11. For complementation of *mmt1* mutants, a 6.2-kb *Xho*I fragment from pSLT1.2 was cloned into pCB1532, which carries a sulfonylurea resistance selectable marker gene (Carroll et al., 1994), and introduced into *mmt1-C6*. Sulfonylurea-resistant transformants were selected, screened by DNA gel blot analysis, and characterized to ensure restoration of the wild-type phenotype.

Plant Infection Assays

Plant infection assays were performed by spraying seedlings of rice (*Oryza sativa*) cultivar CO-39 and barley (*Hordeum vulgare*) cultivar Golden Promise with a suspension of 10^5 conidia mL^{-1} using an artist's airbrush (Talbot et al., 1993). Infection-related development was assessed by incubating conidia on plastic cover slips and allowing appressoria to form after 24 h. Cuticle penetration was measured as described by Chida and Sisler (1987). Sensitivity to protoplasting enzymes was assessed by incubating 48-h-grown mycelium in 12.5 mg mL^{-1} of Glucanex in OM buffer (1.2 M $MgSO_4$ and 10 mM Na_2HPO_4/NaH_2PO_4, pH 5.8) at 30°C for up to 3 h. Aliquots of digested mycelium were removed at intervals and protoplasts counted using a haemocytometer (Corning, Corning, NY).

Preparation of Mmt1 for Chemical Analysis

Mmt1 (MCGDNCTCGASCSCSSCGTHGK) and Mmt2 (MSPATCGCNSCSCASCASCSCCTSCGK) peptides were chemically synthesized by

solid phase synthesis (Affiniti Research, Exeter, UK). Lyophilized, synthetic Mmt1 peptide (5 mg) was incubated with 55 mg of DTT in 20 mM Tris-HCl, pH 8.6, overnight at ambient temperature (Maret, 1994). This apo-form of Mmt1 was titrated to pH 1.0 and separated from DTT and metal ions by applying it to a Sephadex G-50 fine (Sigma G-50-80; St. Louis, MO) column (1 × 30 cm diameter). The column was pre-equilibrated with 10 mM HCl, pH 2, at room temperature overnight and protein eluted with 10 mM HCl at a flow rate of 10 mL/h. The protein was detected spectrophotometrically at 220 nm using a Cary50Bio spectrophotometer (Varian, Palo Alto, CA). Fractions containing Mmt1 were identified by the 2,2-dithiodipyridine (DTDP) assay (see below), combined, and used for subsequent analyses.

To enable metal binding, Mmt1 was incubated in the presence of 750 μM $ZnSO_4$ (99.999%; Sigma). The pH was slowly adjusted to 8.6 with 1 M Tris-HCl, and the fraction placed at −20°C overnight. Raising the pH slowly allows the MT to refold properly while taking up zinc. After incubation, a second gel filtration step was performed to remove excess zinc using the same column as the initial purification. Hepes buffer (20 mM, pH 7.5, Sigma C-7901) was passed through the column, and because this buffer was at a neutral pH, any Zn^{2+} bound to Mmt1 would not be displaced. Fractions were collected as described previously. DTDP assays were performed to determine which fractions contained the protein.

UV/VIS Redox Assays

For the DTDP assay, 20 μL of the fractionated MT was added to 980 μL of DTDP (0.1 M DTDP and 750 μL of formic acid in a total volume of 200 mL) in a glass cuvette. This was incubated for 5 min at room temperature, and the thiol content was established spectrophotometrically at 343 nm, monitoring 2-thiopyridine formation [ε_{343}(2-thiopyridine) = 7600 M^{-1} cm^{-1}]. For the DTNB assay, Mmt1 (2 μM) was incubated with DTNB (100 μM) in Hepes buffer [4-(2-hydroxyethyl)-piperazine-1-ethanesulfonic acid] in the presence of various concentrations of $ZnSO_4$. The reactions were followed spectrophotometrically for 10 min [ε_{412}(TNB) = 13,600 $M^{-1}cm^{-1}$].

Atomic Absorption Spectroscopy

AAS experiments were performed using a Perkin-Elmer AAnalyst 100 (Foster City, CA). Zinc standards ranging from 0.2 to 1.0 ppm were made up from a zinc standard (BDH, Poole, UK) and were used to generate a titration curve of known zinc concentrations versus absorbance at 213.9 nm. The sample to be tested contained 40 μL of zinc-Mmt1, 40 μL of HNO_3, and 3.92 mL of MilliQ water. The acid was added to release bound zinc from the MT. The experiment was repeated three times.

Zinc Transfer Experiments in the Presence of Chromophoric Dyes

To determine the number of zinc ions bound to Mmt1, two analogous experiments were performed. These were the PAR and Zincon zinc release assays, and they were both performed in the same manner (Jacob et al., 1998b). Zinc-bound Mmt1 (0.7 μM) was added to a solution of PAR (100 μM) or Zincon (100 μM) in Hepes buffer (20 mM, pH 7.4). Ebselen (50 μM) was added to initiate zinc release form Mmt1 and monitored spectrophotometrically at 500 nm [PAR, $\varepsilon_{500}(Zn(PAR)_2)$ = 65,000 M^{-1} cm^{-1}) or 620 nm [Zincon, ε_{620}(Zn(Zincon)] = 23,000 $M^{-1}cm^{-1}$) until no further changes were observed (Jacob et al., 1998b). The reverse process [i.e., zinc transfer from the zinc(dye) complex to the apo-form of Mmt1] was also studied to provide additional information about zinc transfer. The $Zn(PAR)_2$ complex was preformed in Hepes (20 mM, pH 7.4) buffer, and decrease in absorbance of this complex was measured upon addition of apo-Mmt1 (2 μM) at 500 nm. This experiment was repeated using Zincon instead of PAR and monitored at 620 nm. To determine the effect of H_2O_2 on metal release from Mmt1, H_2O_2 (1 mM) was added to zinc-bound Mmt1 (2 μM) in the presence of PAR (100 μM) in Hepes buffer (20 mM, pH 7.4). The reaction was monitored spectrophotometrically at 500 nm and readings taken over 90 min. The maximum zinc release from Mmt1 was calculated by incubation of zinc-bound Mmt1 (2 μM) with ebselen (50 μM) under the same experimental conditions.

pH Titration of Mmt1 Polypeptide

The Mmt1 apo-thionein (2 μM) was dissolved in 720 μL of 0.1 M $NaClO_4$. The pH of the solution was adjusted to 1.8 with $HClO_4$ (0.5 M) and $ZnSO_4$ (4 μM) added. At this low pH, the metal would not bind to the MT. The pH was then slowly raised with NaOH (using NaOH stock solutions of 10, 50, and 100 mM) and changes in absorption measured spectrophotometrically (220 nm). It was necessary to increase the pH slowly to detect the small changes in pH, which would result in zinc binding to Mmt1. A micro pH electrode was used to allow pH measurements in 1 mL sample volume (Vasák and Kägi, 1983; Jiang et al., 2000).

Electrochemistry of Mmt1

To determine the redox potential of Mmt1, 7.4 μM (final concentration) of zinc-bound protein was added to KPi buffer (100 mM, pH 7.5, N_2 purged). GSH (68 μM) was tested in the same buffer as reference standard. Measurements were made at a scan rate of 800 mV s^{-1} using a BAS dropping mercury electrode (stationary mode) coupled to an electrochemical analyzer, BAS100B/W (BAS Instruments, Kenilworth, UK). Buffer alone was tested as control.

Immunolocalization of Mmt1

Antisera were raised in New Zealand white SPF rabbits using synthetic Mmt1 and Mmt2 peptides as immunogens. Antisera were purified by caprylic acid/ammonium sulfate precipitation (Thornton, 2001) to provide IgG-enriched preparations, dialyzed against PBS (0.8% NaCl, 0.02% KCl, 0.115% Na_2HPO_4, and 0.02% KH_2PO_4, pH 7.2), and further affinity purified against respective immunogens using peptide-Sepharose immunoaffinity columns. For ELISA, synthetic peptides were reconstituted in bicarbonate buffer, pH 9.6, to contain 1 mg solid mL^{-1} buffer. Protein concentrations were determined by Bio-Rad Bradford protein assay (Hercules, CA), with BSA (Sigma) as standard. Extracts were double diluted into 50 μL of fresh buffer in Immulon II HB microtitre plates (95029370; Thermo Labsystems, Altrincham, UK) and peptides immobilized by incubation for 16 h at 4°C in sealed plastic bags. The wells were washed four times with PBST (PBS + 0.05% [v/v] Tween 20 [polyoxyethylene-sorbitan monolaurate]; P-1379; Sigma), once each with PBS and deionized water and air-dried at 23°C.

Wells containing immobilized peptide were incubated with affinity-purified anti-Mmt1 pAb diluted 1 in 100 in PBST (equivalent to 0.6 μg protein mL^{-1} buffer) for 1 h followed by goat anti-rabbit IgG (whole molecule) peroxidase conjugate (A-6154; Sigma) diluted 1 in 2000 for 1 h. Bound antibody was visualized by incubating with tetramethyl benzidine for 30 min. Reactions were stopped by the addition of 3 M H_2SO_4, and absorbance determined at 450 nm with an MRX automated microplate reader (Dynex Technologies, Billingshurst, UK). Wells were given four 5-min rinses with PBST between incubations. Working volumes were 50 μL per well, and incubation steps were performed at 23°C in sealed plastic bags.

Immunoblotting experiments were performed using protein extracts from lyophilized hyphae that had been grown from conidial suspensions for 48 h. Proteins were extracted as described previously (Thornton, 2001), quantified by Bradford assay (Bio-Rad), and fractionated with 4 to

20% gradient polyacrylamide gels (Bio-Rad) under denaturing conditions. Denatured proteins were prepared by heating at 95°C for 10 min in the presence of β-mercaptoethanol before gel loading. Separated proteins were transferred electrophoretically to a PVDF membrane (Immunoblot-PVDF; Bio-Rad). Membranes were washed three times with PBS and then blocked for 16 h at 4°C with PBS containing 1% (w/v) BSA. Blocked membranes were incubated with a 1/5000 dilution of anti-Mmt1 primary antibody in PBS containing 0.5% BSA for 2 h at 23°C. After washing three times with PBS, membranes were incubated for 1 h with a goat-anti-rabbit alkaline-phosphatase conjugate at 1/15000 dilution. Membranes were washed twice in PBS and once with PBST and bound antibody visualized with substrate solution as described previously (Thornton, 2001)

Immunogold labeling was performed with hyphae, germinating conidia, and mature appressoria of *M. grisea* Guy11. In all cases, biological material was washed twice by centrifugation and resuspended in deionized water. Mycelium was embedded at low temperature in LR White (Cole et al., 1998), except that the resin polymerization steps were performed at 23°C. Immunolabeling was performed essentially as described in Cole et al. (1998) using affinity-purified anti-Mmt1 pAb (diluted in PBST plus 1% BSA to give a final concentration of pAb of 0.03 mg protein mL^{-1} buffer) for 1 h. After thorough rinsing with PBST (four times, 3 min), sections were labeled with goat anti-rabbit 20-nm colloidal gold conjugate (EM.GAR20; British Biocell International, Cardiff, UK), diluted 1 in 20 in PBST plus 1% BSA for 1 h, and washed again with PBST. In the absence of preimmune serum, pAb diluent (PBST/BSA) was used as the control, but grids were otherwise treated the same. During incubation steps, grids were agitated by vibration from an air pump. Sections were post-stained with 2% (w/v) aqueous uranyl acetate (20 min) and lead citrate (4 min) before observation using a JEOL 100S TEM at 80 kV (Tokyo, Japan).

Sequence data from this article have been deposited with the EMBL/GenBank data libraries under accession number AY552780 (*MMT1*).

ACKNOWLEDGMENTS

This work was supported by grants to N.J.T. from the Biotechnology and Biological Sciences Research Council (P18247) and studentships to S.L.T. and M.J.E. C.J. acknowledges support of the Wellcome Trust, the Leverhulme Trust, Royal Society, and the Alzheimer's Society (UK). K.M.T. was supported by an Engineering and Physical Sciences Research Council studentship.

Received January 27, 2004; accepted March 26, 2004.

REFERENCES

Andrews, G.K. (2000). Regulation of metallothionein gene expression by oxidative stress and metal ions. Biochem. Pharmacol. **59,** 95–104.

Andrews, G.K. (2001). Cellular zinc sensors: MTF-1 regulation of gene expression. Biometals **14,** 223–237.

Blindauer, C.A., Harrison, M.D., Parkinson, J.A., Robinson, A.K., Cavet, J.S., Robinson, N.J., and Sadler, P.J. (2001). A metallothionein containing zinc finger within a four-metal cluster protects bacterium from zinc toxicity. Proc. Natl. Acad. Sci. USA **98,** 9593–9598.

Butt, T.R., Sternberg, E.J., Gorman, J.A., Clark, P., Hamer, D., Rosenberg, M., and Crooke, S.T. (1984). Copper metallothionein of yeast, structure of the gene, and regulation of expression. Proc. Natl. Acad. Sci. USA **81,** 3332–3336.

Carroll, A.M., Sweigard, J.A., and Valent, B. (1994). Improved vectors for selecting resistance to hygromycin. Fungal Genet. Newsl. **41,** 22.

Chida, T., and Sisler, H.D. (1987). Restoration of appresorial penetration ability by melanin precursors in *Pyricularia oryzae* treated with antipenetrants and in melanin-deficient mutants. J. Pestic. Sci. **12,** 49–55.

Chumley, F.G., and Valent, B. (1990). Genetic analysis of melanin-deficient, non-pathogenic mutants of *Magnaporthe grisea*. Mol. Plant-Microbe Interact. **3,** 135–143.

Cole, L., Dewey, F.M., and Hawes, C.R. (1998). Immunocytochemical studies of the infection mechanisms of *Botrytis fabae*. I. The fungal extracellular matrix in penetration and post-penetration processes. New Phytol. **139,** 597–609.

Dean, R.A. (1997). Signal pathways and appressorium morphogenesis. Annu. Rev. Phytopathol. **35,** 211–234.

de Jong, J.C., McCormack, B.J., Smirnoff, N., and Talbot, N.J. (1997). Glycerol generates turgor in rice blast. Nature **389,** 244–245.

Fabisiak, J.P., Borisenko, G.G., Liu, S.X., Tyurin, V.A., Pitt, B.R., and Kagan, V.E. (2002). Redox sensor function of metallothioneins. Methods Enzymol. **353,** 268–281.

Fliss, H., and Ménard, M. (1992). Oxidant-induced mobilization of zinc from metallothionein. Arch. Biochem. Biophys. **293,** 195–199.

Galhaup, C., and Haltrich, D. (2001). Enhanced formation of laccase activity by white-rot fungus *trametes pubescens* in the presence of copper. Appl. Microbiol. Biotechnol. **56,** 225–232.

Gustin, M.C., Albertyn, J., Alexander, M., and Davenport, K. (1998). MAP kinase pathways in the yeast *Saccharomyces cerevisiae*. Microbiol. Mol. Biol. Rev. **62,** 1264–1300.

Hahn, M., and Mendgen, K. (1997). Characterisation of *in planta*-induced rust genes isolated from a haustorium-specific cDNA library. Mol. Plant-Microbe Interact. **10,** 427–437.

Hamer, D.H. (1986). Metallothionein. Annu. Rev. Biochem. **55,** 913–951.

Howard, R.J., Ferrari, M.A., Roach, D.H., and Money, N.P. (1991). Penetration of hard substrates by a fungus employing enormous turgor pressures. Proc. Natl. Acad. Sci. USA **88,** 11281–11284.

Hwang, C.-S., and Kolattukudy, P.E. (1995). Isolation and characterization of genes expressed uniquely during appressorium formation by *Colletotrichum gloeosporioides* conidia induced by the host surface wax. Mol. Gen. Genet. **247,** 282–294.

Jacob, C., Maret, C., and Vallee, B.L. (1998b). Control of zinc transfer between thionein, metallothionein and zinc proteins. Proc. Natl. Acad. Sci. USA **95,** 3489–3494.

Jacob, C., Maret, W., and Vallee, B.L. (1998a). Ebselen, a selenium-containing redox drug, releases zinc from metallothionein. Biochem. Biophys. Res. Comm. **248,** 569–573.

Jiang, L.-J., Vasák, M., Vallee, B.L., and Maret, W. (2000). Zinc transfer potentials of the α- and β-clusters of metallothionein are affected by domain interactions in the whole molecule. Proc. Natl. Acad. Sci. USA **97,** 2503–2508.

Kägi, J.H.R. (1993). Metallothionein III. (Basel, Switzerland: Birkhauser).

Lamb, C., and Dixon, R.A. (1997). The oxidative burst in plant disease resistance. Annu. Rev. Plant Physiol. Plant Mol. Biol. **48,** 251–275.

Lanfranco, L., Bolchi, A., Cesale Ros, E., Ottonello, S., and Bonfante, P. (2002). Differential expression of a metallothionein gene during the presymbiotic phase of an arbuscular mycorrhizal fungus. Plant Physiol. **130,** 58–67.

Maret, W. (1994). Oxidative metal release from metallothionein via zinc-thiol/disulfide interchange. Proc. Natl. Acad. Sci. USA **91,** 237–241.

Mellersh, D.G., Foulds, I.V., Higgins, V.J., and Heath, M.C. (2002). H_2O_2 plays different roles in determining penetration failure in three diverse plant-fungal interactions. Plant J. **29,** 257–268.

Münger, K., Germann, U.A., and Lerch, K. (1987). The *Neurospora crassa* metallothionein gene. J. Biol. Chem. **262,** 7363–7367.

Münger, K., and Lerch, K. (1985). Copper metallothionein from the fungus *Agaricus bisporus*: Chemical and spectroscopic properties. Biochemistry **24,** 6751–6756.

Olafson, R.W. (1998). Electrochemical characterization of metallothionein metal mercaptide complexes: Application of cyclic voltammetry to investigation of metalloproteins. Bioelectrochem. Bioenerg. **19,** 111–125.

Palmiter, R.D. (1998). The elusive function of metallothioneins. Proc. Natl. Acad. Sci. USA **95,** 8428–8430.

Pasechnik, T.D., Aver'yanov, A.A., Lapikova, V.P., Kovalenko, E.D., and Kolomietz, T.M. (1998). The involvement of activated oxygen in the expression of the vertical and horizontal resistance of rice to blast disease. Russian J. Plant Physiol. **45,** 371–378.

Sambrook, J., Fritsch, E.F., and Maniatis, T. (1989). Molecular Cloning: A Laboratory Manual. (Cold Spring Harbor, NY: Cold Spring Harbor Laboratory Press).

Shaw, C.F., III, Laib, J.E., Savas, M.M., and Petering, D.H. (1990). Biphasic kinetics of aurothionein formation from gold sodium thiomalate—A novel metallochromic technique to probe Zn^{2+} and Cd^{2+} displacement from metallothionein. Inorg. Chem. **29,** 403–408.

Talbot, N.J. (2003). On the trail of a cereal killer: Exploring the biology of *Magnaporthe grisea*. Annu. Rev. Microbiol. **57,** 177–202.

Talbot, N.J., Ebbole, D.J., and Hamer, J.E. (1993). Identification and characterization of *MPG1*, a gene involved in pathogenicity from the rice blast fungus *Magnaporthe grisea*. Plant Cell **5,** 1575–1590.

Thompson, J.D., Higgins, D.G., and Gibson, T.J. (1994). CLUSTAL W: Improving the sensitivity of progressive multiple sequence alignment through sequence weighting, position-specific gap penalties and weight matrix choice. Nucleic Acids Res. **22,** 4673–4680.

Thornalley, P.J., and Vasák, M. (1985). Possible role for metallothionein in protection against radiation-induced oxidative stress. Kinetics and mechanisms of its reaction with superoxide and hydroxyl radicals. Biochim. Biophys. Acta **827,** 36–44.

Thornton, C.R. (2001). Immunological methods for fungi. In Molecular and Cellular Biology of Filamentous Fungi: A Practical Approach, N.J. Talbot, ed (Oxford, UK: Oxford University Press), pp. 227–257.

Vasák, M., and Hasler, D.W. (2000). Metallothioneins: New functional and structural insights. Curr. Opin. Chem. Biol. **4,** 177–183.

Vasák, M., and Kägi, J.H.R. (1983). Spectropic properties of metallothionein. In Metal Ions in Biological Systems, H. Sigel, ed (New York: Marcel Dekker), pp. 213–273.

Viaud, M.C., Balhadère, P.V., and Talbot, N.J. (2002). A *Magnaporthe grisea* cyclophilin acts as a virulence determinant during plant infection. Plant Cell **14,** 917–930.

Xu, J.-R., and Hamer, J.E. (1996). MAP kinase and cAMP signalling regulate infection structure formation and pathogenic growth in the rice blast fungus *Magnaporthe grisea*. Genes Dev. **10,** 2696–2706.